Luminescence of Ni^{2+} and Cr^{3+} centres in $MgSiO_3$ enstatite crystals

1999 J. Phys.: Condens. Matter 11 6831

(http://iopscience.iop.org/0953-8984/11/35/319)

J. Phys.: Condens. Matter **11** (1999) 6831–6841. Printed in the UK PII: S0953-8984(99)03153-7

Luminescence of Ni^{2+} and Cr^{3+} centres in $MgSiO_3$ enstatite crystals

R Moncorgé†⁺, M Bettinelli‡, Y Guyot§, E Cavalli‖, J A Capobianco¶ and S Girard†

† Centre Interdisciplinaire de Recherche Ions Lasers, UMR 6637 CEA-CNRS-ISMRA, Université de Caen, 14050 Caen, France
‡ Dipartimento Scientifico e Tecnologico, Università di Verona, 37134 Verona, Italy
§ Laboratoire de Physico-Chimie des Matériaux Luminescents, UMR 5620 CNRS, Université de Lyon I, 69622 Villeurbanne, France
‖ Dipartimento di Chimica GIAF, Università di Parma, 43100 Parma, Italy
¶ Department of Chemistry and Biochemistry, Concordia University, Montreal, Quebec H3G 1M8, Canada

E-mail: moncorge@spalp255.ismra.fr

Received 1 April 1999, in final form 25 May 1999

Abstract. Emission and excitation spectra and luminescence decay curves of enstatite $MgSiO_3$ single crystals nominally doped with Ni and Cr have been measured at temperatures down to 10 K. For all the crystals under investigation, the emission band peaking at about 1520 nm is assigned to the $^3T_2 \rightarrow {}^3A_2$ transition of octahedral Ni^{2+} centres, whilst the luminescence around 800 nm is assigned to the $^4T_2 \rightarrow {}^4A_2$ transition of octahedral Cr^{3+} centres. Chemical analysis has confirmed the presence of Ni impurities in the nominally Cr doped crystals, and Cr impurities in the nominally Ni doped crystals. The peak stimulated emission cross section of the 1520 nm emission of Ni^{2+} is 3×10^{-20} cm^2.

1. Introduction

In the case of the recently discovered crystals doped with Cr^{4+} ions such as $Cr:Mg_2SiO_4$ (Cr:forsterite) or $Cr:Y_3Al_5O_{12}$ (Cr:YAG or black garnet), the Cr^{4+} ions are located in tetrahedral or quasi-tetrahedral crystalline environments [1] such that the optical transitions can be electric-dipole allowed thus giving rise to large absorption and emission cross sections. This is the reason why these materials have been shown to be very good broad-band laser systems as well as excellent saturable absorbers for the production of short laser pulses. However, if the stimulated emission cross section of these systems is comparable to that of Ti:sapphire, their fluorescence lifetimes (τ_f) remain short with values of a few microseconds and the resulting $\sigma_e\tau_f$ product is small (where σ_e is the stimulated emission cross section), indicating poor energy storage capabilities.

The ideal situation would be found with a broad-band emitting system having a $\sigma_e\tau_f$ value of a few times 10^{-23} cm^2 s as in the case of Nd:YAG ($\sigma_e\tau_f = 1.6 \times 10^{-23}$ cm^2 s), that is with an emission cross section of a few times 10^{-19} cm^2 and a fluorescence lifetime of a few hundred microseconds.

⁺ Author to whom all correspondence should be addressed. Tel. +33-231-452558. Fax +33-231-452557.

0953-8984/99/356831+11$30.00

It has been shown recently that some Cr doped crystals, crystals having again tetrahedral sites, could fulfil the above requirements. The first example was found with Cr:$LiAlO_2$ [2] which emits a broad band emission around 1300 nm characterized by an estimated stimulated emission cross section at maximum of the order of 3.3×10^{-19} cm^2 with a room temperature fluorescence lifetime of about 29 μs. However, due to the difficulties in the crystal growth, no lasing action of this material has been reported so far. A second example has been found even more recently with Cr:Li_2MgSiO_4 [3] which also emits around 1300 nm with an estimated stimulated emission cross section of about 1.2×10^{-19} cm^2 and a fluorescence lifetime of 100 μs at room temperature. In this case, also, the crystal growth appears to present some difficulties.

The optical spectroscopy of Cr^{3+} in orthoenstatite $MgSiO_3$ was discussed by some of us several years ago [4]. In a recent communication [5], we reported that a Cr doped orthoenstatite $MgSiO_3$ crystal gives rise to a broad-band emission in the eye-safe spectral region around 1.52 μm, with a room-temperature fluorescence lifetime of about 90 μs. This emission was tentatively assigned to thermalized $^3T_2 \rightarrow {}^3A_2$ and $^1E \rightarrow {}^3A_2$ emission transitions in Cr^{4+} centres; however, several doubts concerning the assignment of the optical transitions in the infrared region still remained [5]. For this reason, we decided to undertake a thorough investigation of chemical and physical properties of this material, and chemical analysis showed that our Cr doped orthoenstatite $MgSiO_3$ crystals contained Ni^{2+} impurities. We therefore decided to grow a set of Ni:$MgSiO_3$ crystals, in order to compare the spectroscopy with the data obtained for the crystals with nominal composition Cr:$MgSiO_3$. This comparison allowed us to confidently assign the emission around 1.52 μm in the latter crystals to the $^3T_2 \rightarrow {}^3A_2$ transition of octahedral Ni^{2+} present as unintentional impurity. The results of the detailed spectroscopic investigation are presented in the following sections.

2. Experiment

Crystals of nominal compositions Cr:$MgSiO_3$ (Cr/Mg molar ratio $= 1.0\%$) and Ni:$MgSiO_3$ (Ni/Mg molar ratio $= 1.0$ and 0.10%) were grown by using the flux growth technique in the temperature range 650–950 °C with lithium vanado-molybdate as a solvent [4–7]. The soaking time was about 12 h, the cooling rate 5 °C h^{-1}. The composition of the growing mixture was, in mol%: 6.8 SiO_2, 6.7 MgO, 44.8 Li_2CO_3, 36.6 MoO_3, 5.1 V_2O_5. The appropriate dopants were added as Cr_2O_3, CrO_3 or NiO. All chemicals were reagent grade or better. Growths were carried out in air as well as in oxygen atmosphere. Crystals of more or less pale green or yellow colour, up to $0.5 \times 1 \times 2$ mm^3 in size, were obtained. This size is large enough to measure absorption, excitation and emission spectra and fluorescence decays from room temperature down to about $T = 10$ K. No differences were found in the optical spectra of the crystals grown in air and in oxygen. The actual concentrations of the metals in the samples were determined by inductively coupled plasma (ICP) analysis. The crystals under investigation were found to contain in all cases V (certainly coming from the flux), Ni and Cr. The results of the chemical analysis are reported in table 1. The small amount of Ni present in the nominal Cr:$MgSiO_3$

Table 1. Molar ratios obtained by chemical analysis of the crystals under investigation.

Crystal with nominal ratio	Actual Cr/Mg ratio	Actual Ni/Mg ratio	Actual V/Mg ratio
$Cr/Mg = 1.0 \times 10^{-2}$	8.7×10^{-3}	1.9×10^{-4}	1.6×10^{-3}
$Ni/Mg = 1.0 \times 10^{-2}$	1.8×10^{-4}	1.1×10^{-2}	2.4×10^{-3}
$Ni/Mg = 1.0 \times 10^{-3}$	3.9×10^{-5}	1.4×10^{-3}	1.4×10^{-3}

crystal and the small amount of Cr present in the nominal Ni:$MgSiO_3$ have to be attributed to impurities of unknown origin (such as contamination of the furnace).

The equipment used for the spectroscopic measurements has been described elsewhere [8].

3. Results

The enstatite crystal nominally doped with 1.0% Cr (hereafter E10Cr) was found to emit two well separated emission bands (figures 1 and 2) following excitation at 635 nm and 1200 nm, respectively. One band extends in the red from about 700 to 1100 nm with a maximum around

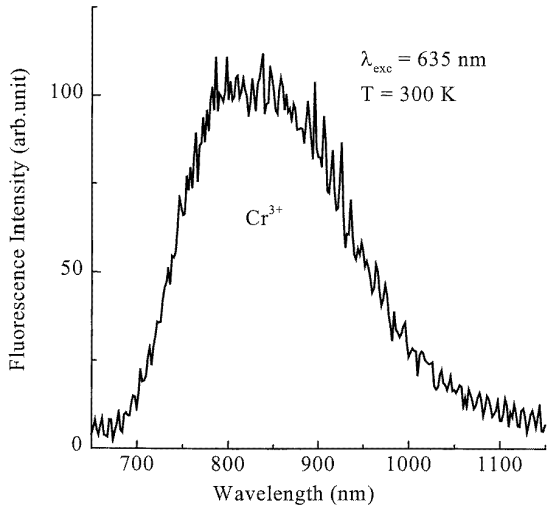

Figure 1. Near infrared emission spectrum of the crystal with nominal composition $MgSiO_3$:1.0%Cr (E10Cr) obtained at room temperature after excitation at 635 nm.

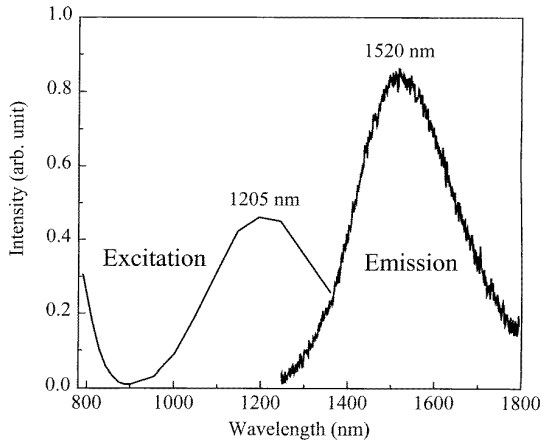

Figure 2. Infrared emission and excitation spectra of the crystal with nominal composition $MgSiO_3$:1.0% Cr (E10Cr) obtained at room temperature with excitation at 1205 nm, and emission at 1500 nm, respectively.

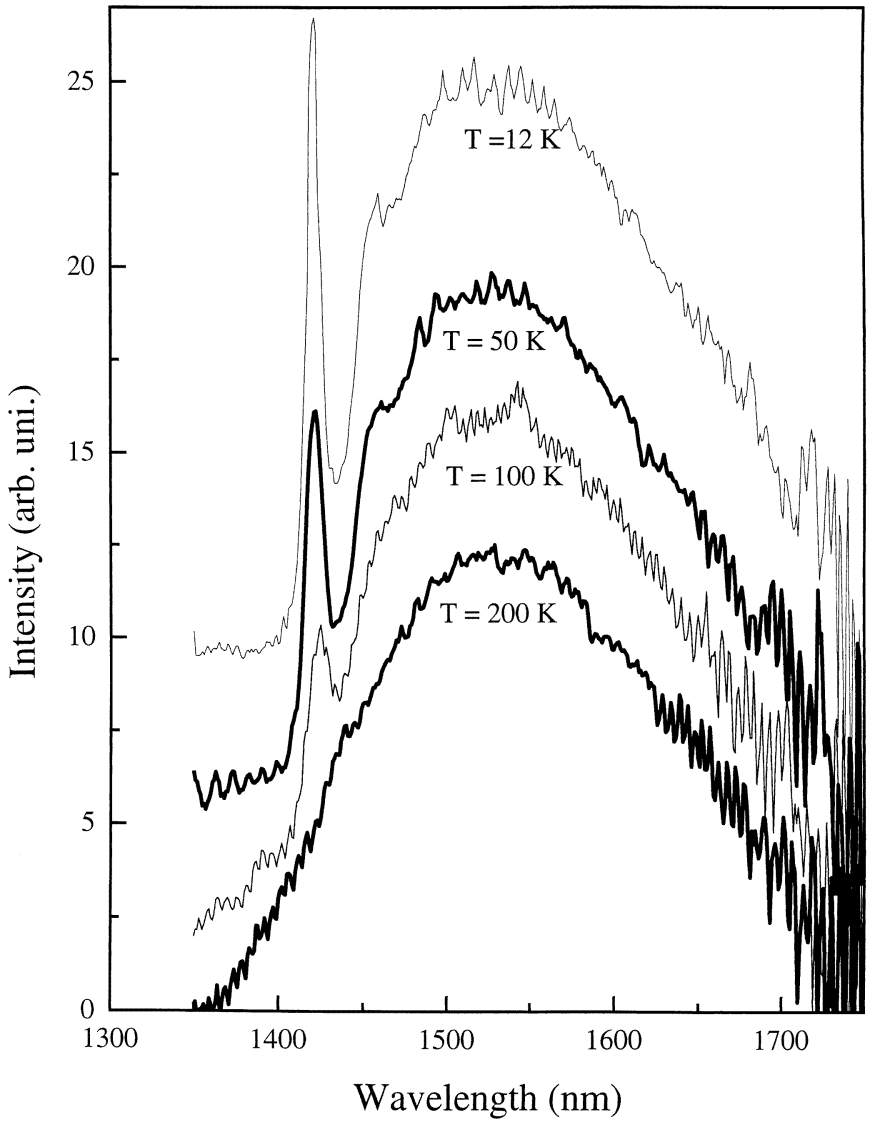

Figure 3. Infrared emission band of the crystal with nominal composition $MgSiO_3$:1.0% Cr (E10Cr) versus temperature.

850 nm and is flanked, at low temperature, by several sharp peaks on its high energy side (see figure 2 of [4]) located around 690 nm, in coincidence with the ones observed in the absorption spectra. The other band extends between 1350 and 1800 nm with a maximum around 1520 nm and is flanked at low temperature by a single sharp peak located on its high energy side around 1420 nm (figure 3).

The first band is made in fact of two overlapping components, one being centred around 780 nm (the one observed after excitation around 470 nm and reported in [4]) and another one peaking around 900 which can be selected and registered by exciting in the near infrared around 790 nm, i.e. in a wavelength domain for which the luminescent centres responsible for the first emission do not absorb.

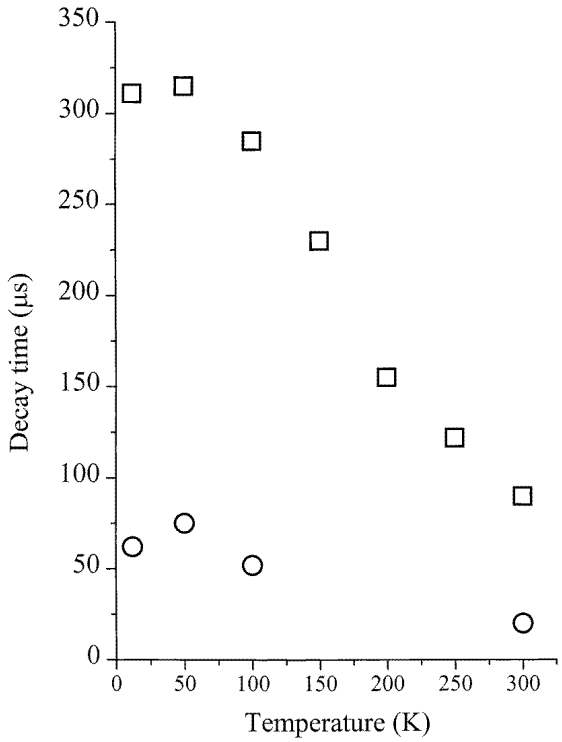

Figure 4. Fluorescence time constants of the 1560 nm emission versus temperature (fluorescence decays are slightly non-exponential and can be decomposed into two components, one dominant long-lived component τ_1 and one weak short-lived component τ_2).

Both broad-band fluorescences decay with time constants of about 35 μs at low temperature ($T = 12$ K) and time constants of about 23 μs for the short-wavelength feature and 35 μs for the long-wavelength one, respectively, at room temperature.

The emission located around 1520 nm is characterized by a broad band and a single sharp line subsisting at fairly high temperature (above 100 K) (figure 3). The same decay constant (300 μs at $T = 10$ K and 90 μs at room temperature) was found for the broad band around 1560 nm and the sharp peak at 1420 nm (figure 4).

Excitation spectra in the region of the sharp line were measured at low and high temperatures. The low-temperature ($T = 12$ K) excitation spectrum shown in figure 5 was recorded with the aid of a Raman shifted pulsed dye laser (spectral width of $\sim$0.2 cm^{-1}) between 1250 and 1450 nm. The excitation spectrum shown in figure 2 was measured at room temperature between 800 and 1350 nm, with the aid of a broad-band optical parametric oscillator (OPO) with a spectral width of 1 nm. The room-temperature excitation spectrum shows the presence of a broad-band absorption peaking around 1205 nm. The low-temperature excitation spectrum shown in figure 5 does not evidence any clear feature coincident with the sharp zero-phonon line, but only a weak peak at about 1380 nm (7250 cm^{-1}).

The luminescence spectra of the enstatite crystals nominally doped with 1.0% and 0.1% Ni (hereafter E10Ni and E01Ni, respectively), obtained at 10 and 300 K with 625 nm excitation, are shown in figures 6 and 7. As in the case of the E10Cr crystal, two

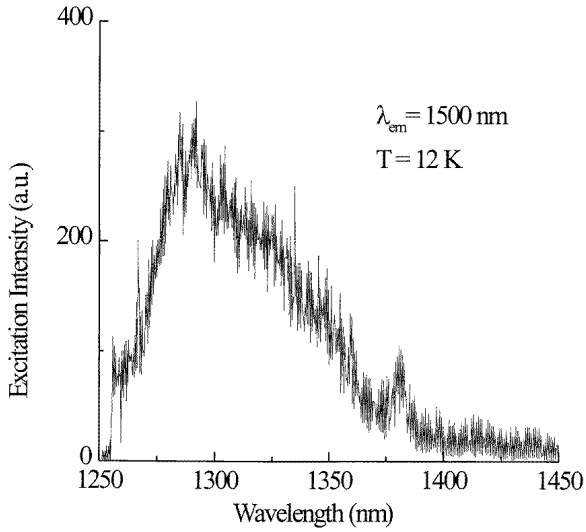

Figure 5. Portion of the low-temperature ($T = 12$ K) excitation spectrum of the infrared emission peaking around 1500 nm (the abrupt cut-off observed at wavelengths shorter than 1285 nm is due to the decreasing dye laser efficiency).

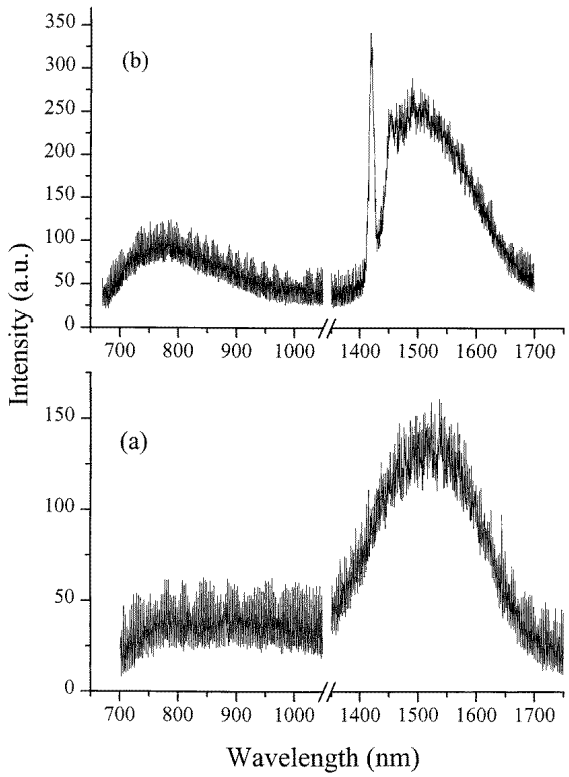

Figure 6. Emission spectra of the crystal with nominal composition $MgSiO_3$:0.10% Ni (E01Ni) after excitation at 625 nm at (a) 300 K and (b) 10 K.

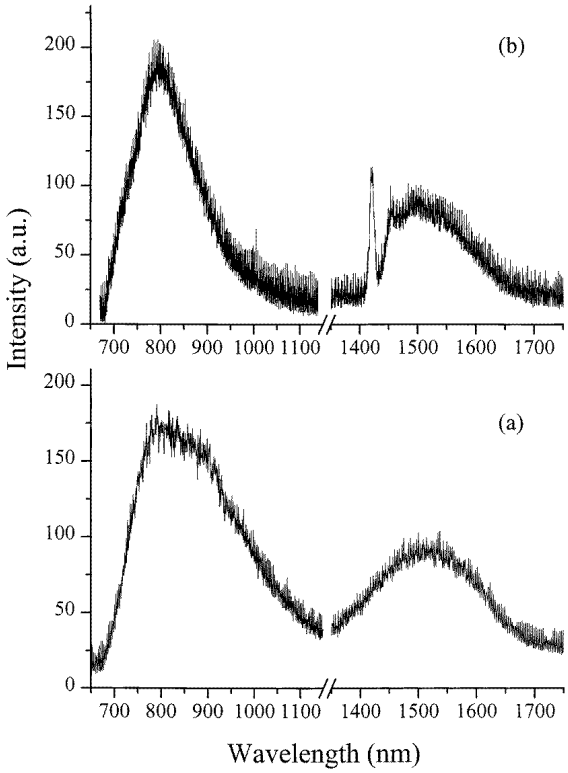

Figure 7. Emission spectra of the crystal with nominal composition $MgSiO_3$:1.0% Ni (E10Ni) after excitation at 625 nm at (a) 300 K and (b) 10 K.

well separated emission bands are present in the spectra. The two bands occur at the same energy in the spectra of the two different crystals, but their relative intensities are different.

Excitation at 625 nm of the E10Ni and E01Ni crystals gives rise to an emission band centred at 780 nm; its relative intensity appears to decrease markedly when the Ni^{2+} concentration is increased. Moreover, we point out that for the E10Ni crystal its intensity decreases significantly with temperature. The position and shape of this band are identical to the corresponding feature for the E10Cr crystal. The band located in the IR peaks at about 1520 nm, and appears to be identical to the band observed in this region for the E10Cr crystal.

For the E10Ni and E01Ni crystals, the decay curves of the 1500 nm emission appear to be dependent both on temperature and on Ni^{2+} concentration (figure 8). For the more diluted crystal E01Ni, the 12 K decay is exponential, with a decay time of 240 μs, whilst the 300 K decay curve is not perfectly exponential, being characterized by a decay time at $1/e$ intensity of 72 μs. For the more concentrated E10Ni crystal, the 12 K decay curve is markedly non-exponential (figure 8), with a decay time at $1/e$ intensity of 27 μs. At 300 K the decay becomes even faster, with a decay time at $1/e$ intensity of 18 μs.

The decay curves of the luminescence at 800 nm are almost exponential for the E01Ni crystal (figure 9), with a decay time close to 35 μs at both 12 and 300 K. In the case of the E10Ni crystal, the decay curves are strongly non-exponential with decay times at $1/e$ intensity of 8 μs at 12 K and 5 μs at 300 K.

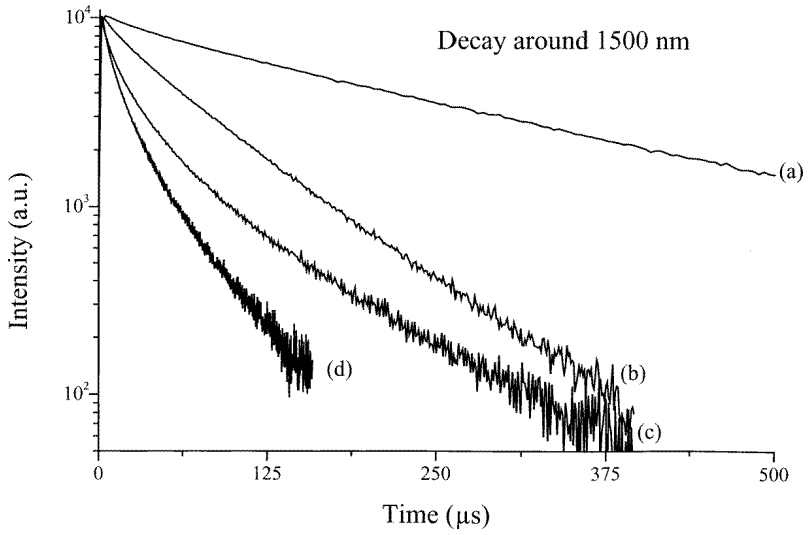

Figure 8. Decay curves of the 1500 nm luminescence for $MgSiO_3$:0.10% Ni (E01Ni) at (a) 12 K and (b) 300 K and for $MgSiO_3$:1.0Ni (E10Ni) at (c) 12 K and (d) 300 K, following pulsed excitation at 625 nm.

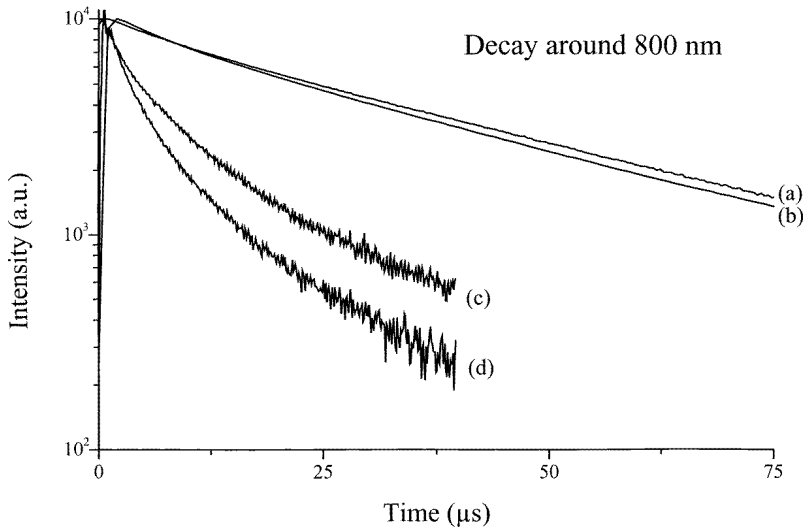

Figure 9. Decay curves of the 800 nm luminescence for $MgSiO_3$:0.10% Ni (E01Ni) at (a) 12 K and (b) 300 K and for $MgSiO_3$:1.0Ni (E10Ni) at (c) 12 K and (d) 300 K, following pulsed excitation at 625 nm.

4. Discussion

4.1. 800 nm luminescence

The spectral features observed in the near infrared spectra of the E10Cr crystal can be assigned to different types of Cr^{3+} ion in (near) octahedral symmetry crystal fields of intermediate and

low strengths [8]. Indeed, the low-pressure form of orthoenstatite $MgSiO_3$ is orthorhombic, space group *Pbca* [9] with lattice parameters $a = 18.21$, $b = 8.812$ and $c = 5.178$ Å. The unit cell contains two sets of non-equivalent Mg^{2+} ions, occupying distorted octahedral sites both of C_1 symmetry, for which the Cr^{3+} dopant ions can substitute. The behaviour is therefore similar to that observed for Cr^{3+} in Mg_2SiO_4 (forsterite) [8] and in the non-stoichiometric green spinel [10].

The fluorescence decay measurements also agree with this interpretation. Indeed, the values observed for the E10Cr crystal are essentially the same as the temperature independent fluorescence time constants of 23 and 35 μs associated with the broad-band emissions of the Cr^{3+} ions in the low-field Mg sites of rhombic symmetry (Cr^{3+} ions having a nearest-neighbour cation vacancy in the [001] direction) evidenced in the past in Cr:$MgAl_2O_4$ [10] and Cr:MgO [11], respectively.

Luminescence in the near infrared (800–1000 nm) has been observed in the past for several Ni^{2+} doped oxide crystals [12, 13] and it has been assigned to the $^1T_2 \rightarrow {}^3T_2$ transition. However, in the case of the E01Ni and E10Ni crystals, this emission would have been the result of an excited state absorption process [14], which is not the case, as moderate power excitation at 625 nm (16 000 cm^{-1}) does not populate the $^1T_2$ state, lying above 20 000 cm^{-1}. For this reason, it does not seem reasonable to attribute the observed emission to Ni^{2+} centres. We point out that the luminescence bands peaking at 780 nm of the E01Ni and E10Ni crystals are similar to the features observed in the same spectral region for E10Cr. Since the Ni doped samples have been found to contain impurities of Cr, it is conceivable that these emission bands are to be assigned to the $^4T_2 \rightarrow {}^4A_2$ transition of Cr^{3+} in enstatite discussed above. In the case of the crystal more strongly concentrated in Ni (E10Ni) the low relative intensity of this band at 12 K is attributed to $Cr^{3+} \rightarrow Ni^{2+}$ energy transfer, quenching the luminescence around 800 nm. This energy transfer process is probably temperature dependent, as the quenching appears to be severely increased at 300 K. In the spectra of E01Ni, the Cr^{3+} emission is strong, probably because at this doping level the quenching induced by Ni^{2+} is not efficient.

This interpretation is corroborated by the decay curves of the 800 nm luminescence (figure 9). In fact, these results obtained for E01Ni and E10Ni agree with energy transfer processes quenching the luminescence from the $^4T_2$ of the Cr^{3+} impurities in the more concentrated crystal.

4.2. 1500 nm luminescence

The emission located around 1520 nm of the E10Cr crystal is well beyond the emission range of any low-field Cr^{3+} ion so it was tentatively associated with the presence of Cr^{4+} ions in tetrahedral sites, as in the case of Cr:forsterite [8] and, possibly, of Cr:Li_2MgSiO_4 [3]. There are, however, two fundamental differences, compared with Cr:forsterite. First of all, the emission spectrum is characterized by a broad band and a single sharp line subsisting at fairly high temperature (above 100 K) (figure 3). Moreover, the measured lifetime is very long, 300 μs at $T = 10$ K and 90 μs at room temperature (figure 4), compared to that found in the previously investigated Cr^{4+} systems (2.7 μs in the case of Cr:forsterite [1] and 4.1 μs in the case of Cr:YAG [15], for example).

The same decay constant value was found for the broad band around 1560 nm and the sharp peak at 1420 nm: this should indicate that they are associated with the same emitting centre. In Cr:Li_2MgSiO_4 a similar situation was observed and the broad band and the sharp peak were tentatively assigned to thermalized $^3T_2 \rightarrow {}^3A_2$ and $^1E \rightarrow {}^3A_2$ emission transitions, respectively [3].

The low-temperature excitation spectrum shown in figure 5 does not evidence any clear feature coincident with the sharp zero-phonon line, but only a weak peak at about 1380 nm (7250 cm^{-1}).

This last observation makes the possible assignment of the near-infrared luminescence to thermalized $^3T_2 \rightarrow {}^3A_2$ and $^1E \rightarrow {}^3A_2$ emission transitions of Cr^{4+} somewhat doubtful. Since the chemical analysis showed the presence of unintentional Ni impurities, an alternative explanation would be that the emission around 1520 nm is related to the presence of Ni^{2+} octahedral centres, which are known to emit at this wavelength [12, 16].

In the case of luminescence spectra of the enstatite crystals E10Ni and E01Ni the band located in the IR peaks at about 1520 nm appears to be identical to the band observed in this region for the E10Cr crystal. Moreover, the shape and position of these spectral features are very similar to the 1500 nm emission band, assigned to the $^3T_2 \rightarrow {}^3A_2$ transition of octahedral Ni^{2+}, in the case of Ni:Mg_2SiO_4 (Ni:forsterite) [12]. These analogies suggest that for all the crystals under investigation the sharp line and the broad band around 1520 nm are assigned to a $Ni^{2+}(O_h)$ $^3T_1 \rightarrow {}^3A_2$ transition. It is remarkable that in the case of E10Cr a 110 ppm Ni impurity (by weight) gives rise to a transition dominating this spectral region.

The excitation spectrum of the 1500 nm emission of the E10Cr crystal (figures 2 and 5) is similar to the one obtained for Ni:Mg_2SiO_4 [12] and is assigned to the reverse $^3T_2 \rightarrow {}^3A_2$ transition of octahedral Ni^{2+}. In our case a zero-phonon line could not be evidenced in the excitation spectrum at 7040 cm^{-1}, but we note that also in the case of forsterite [12] the zero-phonon line at 7280 cm^{-1} appeared to be relatively weak in the excitation spectrum. The shift to low energy of the zero-phonon line on moving from forsterite to enstatite might indicate that Ni^{2+} experiences in the latter a weaker crystal field.

In the case of the E10Cr crystal, in which the concentration of Ni^{2+} is very small (table 1), the lifetime of the $^3T_2$ state is 300 μs at 10 K, decreasing to 90 μs at 300 K. The 10 K value is markedly shorter than the one observed by Walker *et al* (1.2 ms) for the corresponding transition in Ni:Mg_2SiO_4 [12] at low temperature; this difference is attributed to a more distorted symmetry of the optically active Ni^{2+} ions in enstatite [4, 12]. In fact, the contribution to the distortion modulus [17], which measures how much the structural perturbations remove the inversion symmetry, has values 0.0690 and 0.3056 for the Mg(I) and Mg(II) sites of $MgSiO_3$, respectively, and 0 and 0.2615 for the Mg(C_i) and Mg(C_s) sites of Mg_2SiO_4, respectively. The electric dipole transition probability is therefore expected to be higher for Ni^{2+} in enstatite than in forsterite.

The decay curve of the 1500 nm emission from the $^3T_2$ state of octahedral Ni^{2+} centres at 300 K is not perfectly exponential in E01Ni, and it is shorter than at 12 K. A significant shortening of the decay is expected to be induced by multiphonon relaxation; however some temperature dependent concentration quenching effects are probably present at this doping level, as shown by the weakly non-exponential shape of the decay curve. For comparison purposes, the decay time observed at 300 K for Ni:forsterite is about 300 μs [12].

For the more concentrated E10Ni crystal, the 12 K decay curve is markedly non-exponential (figure 8). In this case, the presence of concentration quenching is obvious. At 300 K the decay becomes even faster, presumably due to thermally activated concentration quenching processes.

5. Laser potential

Based on the results discussed above, we calculated the stimulated emission cross section σ_e of the infrared emission of Ni^{2+} ions in enstatite $MgSiO_3$. We used the usual equation

$$\sigma_e(\lambda) = \frac{\lambda^5}{8\pi n^2 c \tau_r} \frac{I(\lambda)}{\int \lambda I(\lambda)\, d\lambda}$$

where c is the velocity of light, n the refractive index, τ_r the radiative lifetime of the emitting level and $I(\lambda)$ is the emission intensity. We assumed $n = 1.65$, i.e. a value close to the one pertinent to the similar host Mg_2SiO_4, and we took for the radiative lifetime the value $\tau_r = 300\ \mu$s, corresponding to the decay time of the $^3T_2 \rightarrow {}^3A_2$ transition at 10 K in the very diluted E10Cr crystal (see above). σ_e peaks around 1550 nm, with a maximum value of 3×10^{-20} cm^2. Due to the significantly smaller value of the radiative lifetime, induced by the distortion of the Ni^{2+} sites discussed above, the cross section in $MgSiO_3$ is roughly one order of magnitude higher than observed for Ni^{2+} in crystals like MgO and MgF_2 [13]. In the present case, $\tau_f(300\ \text{K}) = 90\ \mu$s and $\sigma_e = 3 \times 10^{-20}$ cm^2; this situation is comparable to what was found for the important laser crystal Cr^{3+}:$LiCaAlF_6$ (LiCAF), for which $\tau_f(300\ \text{K}) = 170\ \mu$s and $\sigma_e = 1.3 \times 10^{-20}$ cm^2 [18]. This result appears to be promising. However, it has to be considered that the shortening of the decay time indicates that the luminescence quantum efficiency at room temperature is about 30%, and that concentration quenching appears to occur. Moreover, the effect of excited state absorption will have to be carefully examined.

6. Conclusions

The luminescence spectroscopy of enstatite $MgSiO_3$ single crystals intentionally doped with both Cr or Ni appears to be strongly influenced by the presence of unintentional impurities. Chemical analysis has shown the presence in all the crystals under investigation of Cr, Ni and V. Whereas this last impurity clearly originates from the vanado-molybdate flux employed in the crystal growth, and appears to be present as VO_4^{3-} ions [4], the occurrence of Ni^{2+} luminescence in Cr:$MgSiO_3$ and Cr^{3+} luminescence in Ni:$MgSiO_3$ has given rise to unexpected features in the optical spectra. We point out that the crystals under investigation were grown using reagent grade starting materials and that the presence of impurities (a few hundred ppm in weight) was sufficient to originate strong luminescence bands, in particular in the case of the 1500 nm emission band of Ni^{2+}.

The laser potential of Ni:$MgSiO_3$ around 1500 nm appears to be promising, as $\sigma_e\tau_f = 2.7 \times 10^{-24}$ cm^2 s. In this regard, we point out that it is possible to grow $MgSiO_3$ crystals of size $6 \times 4 \times 5$ mm^3 using the top-seeded solution growth method [6].

References

[1] Moncorgé R, Manaa H and Boulon G 1994 *Opt. Mater.* **4** 139
[2] Kück S, Hartung S, Petermann K and Huber G 1995 *Appl. Phys.* B **61** 33
[3] Anino C, Théry J and Vivien D 1997 *Opt. Mater.* **8** 121
[4] Cavalli E and Bettinelli M 1993 *Opt. Mater.* **2** 151
[5] Moncorgé R, Capobianco J A, Bettinelli M, Cavalli E, Girard S and Guyot Y 1998 *Advanced Solid State Lasers (OSA TOPS 19)* ed W R Bosenberg and M J Fejer (Optical Society of America) p 484
[6] Tanaka T and Takei H 1997 *J. Cryst. Growth* **180** 206
[7] Grandin de l'Epervier A and Ito J 1983 *J. Cryst. Growth* **64** 411
[8] Moncorgé R, Cormier G, Simkin D J and Capobianco J A 1991 *IEEE J. Quant. Electron.* **27** 114
[9] Morimoto N and Koto K 1969 *Z. Kristallogr.* **129** 65
[10] Garapon C, Manaa H and Moncorgé R 1991 *J. Chem. Phys.* **95** 5501
[11] Henry M O, Larkin J P and Imbusch G F 1976 *Phys. Rev.* B **13** 1893
[12] Walker G, Kamaluddin B, Glynn T J and Sherlock R 1994 *J. Lumin.* **60/61** 123
[13] Moncorgé R and Benyattou T 1988 *Phys. Rev.* B **37** 9186
[14] Moncorgé R, Auzel F and Breteau J M 1985 *Phil. Mag.* B **51** 489
[15] Kück S 1994 *PhD Thesis* University of Hamburg
[16] Moncorgé R 1989 *Proc. SPIE* **1182** 34
[17] Cammi R and Cavalli E 1992 *Acta Crystallogr.* B **48** 245
[18] Payne S A, Chase L L, Newkirk H W, Smith L K and Krupke W F 1988 *IEEE J. Quantum Electron.* **24** 2243